

# A tailored next-generation sequencing panel identified distinct subtypes of wildtype IDH and TERT promoter glioblastomas

Nayuta Higa<sup>1</sup> | Toshiaki Akahane<sup>2,3</sup> | Seiya Yokoyama<sup>2</sup> | Hajime Yonezawa<sup>1</sup> | Hiroyuki Uchida<sup>1</sup> | Tomoko Takajo<sup>1</sup> | Mari Kirishima<sup>2</sup> | Taiji Hamada<sup>2</sup> | Kei Matsuo<sup>2</sup> | Shingo Fujio<sup>1</sup> | Tomoko Hanada<sup>1</sup> | Hiroshi Hosoyama<sup>1</sup> | Masanori Yonenaga<sup>1</sup> | Akihisa Sakamoto<sup>1</sup> | Tsubasa Hiraki<sup>2</sup> | Akihide Tanimoto<sup>2,3</sup>  | Koji Yoshimoto<sup>1</sup> 

<sup>1</sup>Department of Neurosurgery, Graduate School of Medical and Dental Sciences, Kagoshima University, Kagoshima, Japan

<sup>2</sup>Department of Pathology, Graduate School of Medical and Dental Sciences, Kagoshima University, Kagoshima, Japan

<sup>3</sup>Center for Human Genome and Gene Analysis, Kagoshima University Hospital, Kagoshima, Japan

## Correspondence

Akihide Tanimoto, Department of Pathology, Graduate School of Medical and Dental Sciences, Kagoshima University, Japan.  
Email: akit09@m3.kufm.kagoshima-u.ac.jp

Koji Yoshimoto, Department of Neurosurgery, Graduate School of Medical and Dental Sciences, Kagoshima University, Japan.  
Email: kyoshimo@m.kufm.kagoshima-u.ac.jp

## Abstract

Central nervous system tumors are classified based on an integrated diagnosis combining histology and molecular characteristics, including *IDH1/2* and *H3-K27M* mutations, as well as 1p/19q codeletion. Here, we aimed to develop and assess the feasibility of a glioma-tailored 48-gene next-generation sequencing (NGS) panel for integrated glioma diagnosis. We designed a glioma-tailored 48-gene NGS panel for detecting 1p/19q codeletion and mutations in *IDH1/2*, *TP53*, *PTEN*, *PDGFRA*, *NF1*, *RB1*, *CDKN2A/B*, *CDK4*, and the *TERT* promoter (*TERTp*). We analyzed 106 glioma patients (grade II: 19 cases, grade III: 23 cases, grade IV: 64 cases) using this system. The 1p/19q codeletion was detected precisely in oligodendroglial tumors using our NGS panel. In a cohort of 64 grade IV gliomas, we identified 56 *IDH*-wildtype glioblastomas. Within these *IDH*-wildtype glioblastomas, 33 samples (58.9%) showed a mutation in *TERTp*. Notably, *PDGFRA* mutations and their amplification were more commonly seen in *TERTp*-wildtype glioblastomas (43%) than in *TERTp*-mutant glioblastomas (6%) ( $P = .001$ ). Hierarchical molecular classification of *IDH*-wildtype glioblastomas revealed 3 distinct groups of *IDH*-wildtype glioblastomas. One major cluster was characterized by mutations in *PDGFRA*, amplification of *CDK4* and *PDGFRA*, homozygous deletion of *CDKN2A/B*, and absence of *TERTp* mutations. This cluster was significantly associated with older age ( $P = .021$ ), higher Ki-67 score ( $P = .007$ ), poor prognosis ( $P = .012$ ), and a periventricular tumor location. We report the development of a glioma-tailored NGS panel for detecting 1p/19q codeletion and driver gene mutations on a single platform. Our panel identified distinct subtypes of *IDH*- and *TERTp*-wildtype glioblastomas with frequent *PDGFRA* alterations.

**Abbreviations:** *ATM*, ataxia telangiectasia-mutated serine/threonine kinase gene; *ATRX*, *ATRX* chromatin remodeler gene; *BRAF*, B-Raf proto-oncogene, serine/threonine kinase gene; *CDK4*, cyclin dependent kinase 4 gene; *CDKN2A/B*, cyclin dependent kinase inhibitor 2A/B gene; CGH, comparative genomic hybridization; cIMPACT-NOW, The Consortium to Inform Molecular and Practical Approaches to CNS Tumor Taxonomy; CISH, chromogenic in situ hybridization; CNS, central nervous system; CNV, copy number variation; *EGFR*, epidermal growth factor receptor gene; FFPE, formalin-fixed and paraffin-embedded; *FUBP1*, far upstream element binding protein 1 gene; GBM, glioblastoma; *IDH*, isocitrate dehydrogenase; *MAP2K4*, mitogen-activated protein kinase 4 gene; MLPA, multiplex ligation-dependent probe amplification; *NF1*, neurofibromin 1 gene; NGS, next-generation sequencing; *PDGFRA*, platelet derived growth factor receptor alpha gene; *PTEN*, phosphatase and tensin homolog; *RB1*, retinoblastoma transcriptional corepressor 1 gene; *TERT*, telomerase reverse transcriptase gene; *TERTp*, telomerase reverse transcriptase gene promoter; *TP53*, tumor protein p53 gene; WHO, World Health Organization.

This is an open access article under the terms of the Creative Commons Attribution-NonCommercial License, which permits use, distribution and reproduction in any medium, provided the original work is properly cited and is not used for commercial purposes.

© 2020 The Authors. *Cancer Science* published by John Wiley & Sons Australia, Ltd on behalf of Japanese Cancer Association.

## KEYWORDS

1p/19q codeletion, glioblastoma, next-generation sequencing, *PDGFRA* alterations, *TERT* promoter

## 1 | INTRODUCTION

The standard method for diagnosing CNS tumors has changed from a histology-based approach to an integrated histology and molecular characteristics-based approach following the implementation of the revised 2016 WHO classifications and their subsequent update by The Consortium to Inform Molecular and Practical Approaches to CNS Tumor Taxonomy (cIMPACT-NOW).<sup>1-7</sup> In this integrated diagnosis, genetic mutations in isocitrate dehydrogenase 1 or 2 (*IDH1* or *IDH2*), codeletion of chromosomal arms 1p and 19q (1p/19q codeletion), and the *H3-K27M* mutation must be evaluated. Other numerous genetic mutations are known to play an important role in gliomas such as mutations in *PTEN* and the epidermal growth factor receptor (*EGFR*) gene, which may serve as diagnostic, prognostic, and therapeutic biomarkers.<sup>8-10</sup>

Currently, diagnostic neuropathology laboratories test for selected biomarkers individually, including mutations in *IDH1/2*, the *ATRX* chromatin remodeler gene (*ATRX*), the telomerase reverse transcriptase gene (*TERT*), *H3-K27M*, and the B-Raf proto-oncogene, serine/threonine kinase gene (*BRAF*), as well as 1p/19q codeletion. This involves various testing methods, including immunohistochemistry with mutation-specific antibodies such as those against *IDH1-R132H*, *BRAF-V600E*, and *H3-K27M*,<sup>11-13</sup> conventional Sanger sequencing or pyrosequencing of tumor DNA for detection of mutations, FISH, CGH, chromogenic in situ hybridization (CISH), PCR-based microsatellite analysis, real-time comparative quantitative PCR; and multiplex ligation-dependent probe amplification for detection of 1p/19q codeletion.<sup>14-18</sup> Immunohistochemical (IHC) assays for *IDH1-R132H*, *BRAF-V600E*, and *H3-K27M* are relatively sensitive and specific, but there is a non-trivial rate of discordance. In addition, a significant proportion of patients harbor other mutations in these genes that are not detectable by IHC, potentially limiting the utility of IHC screening. In the case of 1p/19q codeletion, the most common diagnostic tool is FISH. However, this test can yield false-positive results because commercially available FISH probes are typically designed to target the 1p36 and 19q13 regions and cannot discriminate between whole- and partial-arm chromosome loss.<sup>19</sup> High-throughput array technologies such as CGH is a "whole-genome" array that detects DNA CNVs at multiple sites simultaneously.<sup>14</sup> However, it is cost-prohibitive and therefore not suitable for routine molecular diagnoses in the clinic. To solve these problems, NGS is increasingly used in the diagnostic routine of leading oncology centers. NGS panels allow simultaneous assessment of several mutations and CNVs.

Several targeted NGS panels are available commercially; however, most are designed to identify important alterations in a broad

spectrum of cancers but not glioma specifically.<sup>20,21</sup> Several customized gene panels have been established but they are unable to detect whole chromosome loss of 1p and 19q or do not cover enough driver genes.<sup>22-26</sup> Therefore, we constructed a glioma-tailored 48-gene NGS panel for detecting 1p/19q codeletion and mutations as a routine molecular diagnostic tool for gliomas. Our NGS panel integrates molecular barcode technology into a single gene-specific, primer-based target enrichment process, with clear discrimination of false positives from true positives. This results in both greater sensitivity and greater accuracy in the detection of variants. Molecular barcoding technology aims to reduce the impact of enrichment and sequencing artifacts and has the potential to improve mutation detection accuracy.<sup>27,28</sup>

This novel assay paves the way toward simultaneous detection of both allelic imbalances and mutations in small amounts of DNA retrieved from FFPE tissue samples for glioma subtype diagnostics. In this study, we describe the application of a glioma-tailored 48-gene NGS panel-based analysis of 106 gliomas and evaluate the feasibility by routine molecular diagnostics. Our panel identified distinct subtypes of *IDH*- and *TERTp*-wildtype glioblastomas with frequent *PDGFRA* alterations.

## 2 | MATERIALS AND METHODS

### 2.1 | CNS tumor samples

In total, 106 FFPE tumor tissue samples from 106 patients were selected from the CNS tumor tissue bank at Kagoshima University Hospital. In 5 patients, 2 samples were obtained at different time points and in 1 patient, 3 samples were obtained at different time points. The study was approved by the Institutional Review Board of Kagoshima University and it complied with the Helsinki Declaration. Informed consent was obtained from each patient. Resected tumors were fixed with phosphate-buffered 10% formalin within 24 h and routinely processed for paraffin embedding, followed by sectioning for hematoxylin and eosin staining. All tumors were originally classified according to the WHO classification of 2016. The tumor series consisted of 9 diffuse grade II astrocytomas (A II); 14 grade III anaplastic astrocytomas (AA III); 58 grade IV glioblastomas (GBM IV), including 2 secondary glioblastomas; 10 grade II oligodendrogliomas (O II); 9 grade III anaplastic oligodendrogliomas (AO III); and 6 grade IV diffuse midline gliomas (DMG IV). Supporting Information Table S1 provides an overview of the relevant clinical and histological data of the 106 patients investigated. All tissues were histologically evaluated by board-certified pathologists (MK, TH, and AT) to ensure an estimated tumor cell content of 30% or more, from which DNA was

extracted. In 9 samples, the results were obtained from stereotactic biopsy specimens and in 97 samples the results were obtained in larger tumor resection specimens. In all patients, when analyzing CNVs, we sequenced leukocyte DNA for comparison against the matched tumor DNA.

## 2.2 | DNA extraction and quantification

For DNA preparation from FFPE samples, we used the Maxwell 16 FFPE Tissue LEV DNA Purification kit (Promega) according to the manufacturer's instruction. Leukocyte DNA was extracted from samples from 106 patients with the DNeasy Blood & Tissue Kit (QIAGEN). Afterward, the concentration of DNA was measured using a Qubit 3.0 Fluorometer dsDNA BR assay kit (Life Technologies), DNA quality was monitored by QIAseq DNA QuantIMIZE kits (QIAGEN). The extracted DNA was diluted to a concentration of 5-10 ng/ $\mu$ L as a template, and PCR was performed using the QIAseq DNA QuantIMIZE kits.

## 2.3 | Design of the glioma-tailored 48-gene NGS panel

The customized gene panel for 48 glioma-associated genes was created using the QIAseq (QIAGEN) targeted DNA panels (Figure 1). These 48 genes included the most commonly mutated genes in gliomas as well as genes previously suggested as diagnostically relevant molecular markers, such as *IDH1/2*, *ATRX*, the

capicua transcriptional repressor gene (*CIC*), the *TERT* promoter (*TERTp*), and *BRAF* (Figure 1). For detection of 1p/19q codeletion, we analyzed the CNVs of chromosome 1p loci 9 genes, chromosome 1q loci 5 genes, chromosome 19p loci 5 genes, and chromosome 19q loci 5 genes (Figure 1). The final NGS panel consisted of 1954 primer pairs covering (99.95%) the coding sequences of 48 genes, and *TERTp* regions.

## 2.4 | Library preparation and NGS

Blood and FFPE DNA were treated to construct the NGS library using the QIAseq Custom Brain Tumor Panel (QIAGEN) (glioma-tailored 48-gene NGS panel), also applied to produce the NGS library. In total, 40 (blood) and 100-200 (FFPE) ng DNA for the QIAseq Custom Brain Tumor Panel were used for library construction and were processed with a MiSeq sequencer (Illumina) after dilution with hybridization buffer to a DNA concentration of 20 pmol/L.

## 2.5 | Analysis of NGS data for sequence variants and copy number changes

Amplicon sequences were aligned to the human reference genome GRCh37 (hg19) in the target region of the sequence. Data were analyzed using the QIAGEN Web Portal service (<https://www.qiagen.com/us/shop/genes-and-oathways/data-analysis-center-overview-page/>).

Target genes			
NF1	ACVR1	TNFRSF14 (1p36.32)	STK11 (19p13.3)
ATRX	HIST1H3B	MTOR (1p36.22)	GNA11 (19p13.3)
BRAF	HIST1H3C	SDHB (1p36.13)	MAP2K2 (19p13.3)
CDKN2A	TP53	ARID1A (1p36.11)	SMARCA4 (19p13.2)
CDKN2B	MAP2K4	MUTYH (1p34.1)	JAK3 (19p13.11)
EGFR	CDK12	JAK1 (1p31.3)	CCNE1 (19q12)
IDH1	ATM	FUBP1 (1p31.1)	AKT2 (19q13.2)
IDH2	CCND1	FAM46C (1p12)	AXL (19q13.2)
MDM2	CDK4	NOTCH2 (1p12)	CIC (19q13.2)
PDGFRA	CDK6	DDR2 (1q23.3)	PPP2R1A (19q13.41)
PTEN		NFASC (1q32.1)	
RB1		ESRRG (1q41)	
TERT		H3F3A (1q42.12)	
FGFR1		FH (1q43)	

     Chromosome 1     
      Chromosome 19

**FIGURE 1** Glioma-tailored 48-gene next-generation sequencing (NGS) panel design

## 2.6 | FISH

A *PDGFRA* amplification test was performed on a 4- $\mu$ m FFPE tissue section. The FISH probes used were bacterial artificial chromosome clones RP11-231C18 (*PDGFRA* gene, 4q12) and control probes (4p11, CHR4-10-GR); (all from Empire Genomics). All FISH experimental procedures were performed according to the manufacturer's instructions. Preparations were counterstained with 4,6-diamidino-phenyl-indole (DAPI).

## 2.7 | Array-CGH

Genomic DNA was extracted from whole blood samples using a DNeasy Blood & Tissue Kit (QIAGEN) and 1  $\mu$ g of each sample was labeled using an Agilent SureTag DNA Labeling Kit (Agilent Technologies) and hybridized on an Agilent SurePrint G3 Human CGH Microarray 4  $\times$  180 k (design ID 085723; Agilent Technologies), following the manufacturer's protocol.

## 2.8 | Analysis of array data

Slides were scanned using an Agilent Autofocus Dynamic Scanner (Agilent Technologies) and quantified using Agilent's Feature Extraction software (v10.10.0.23). Quantitative data were loaded into CytoGenomics Software 5.0 (Agilent Technologies) and analyzed using the Aberration Detection Method 2 (ADM2) statistical algorithm at a threshold of 6.0 to identify genomic intervals with copy number changes. To reduce false-positive calls, a filter was applied to define the minimum  $\log_2$  ratio (0.25), and the minimum number of probes.

## 2.9 | Statistical analyses

Unsupervised average linkage hierarchical clustering was applied to the NGS data obtained from the tumors based on Jaccard's matching coefficient to calculate distances. This analysis was performed using R open source statistical computing language (v3.5.3) and the integrated development environment RStudio (v0.99.484) as well as the R packages NMF (v0.20.6), MASS (v7.3-51.5) and STATS (v3.2.2). Cluster analysis was performed using Euclidean distance and Ward.D2 linkage. Other statistical analyses were performed using a JMP Pro v13 software (SAS Institute). Differences were considered significant at  $P < .05$ .

## 3 | RESULTS

### 3.1 | Detection of 1p/19q codeletion

A codeletion of 1p/19q was identified when all of the following conditions were satisfied: a copy number loss of all genes on 1p (9 genes) and 19q (5 genes); (average CNVs of chromosome 1q loci 5 genes)/(average CNVs of chromosome 1p loci 9 genes)  $\geq 2$ ; and (average CNVs of chromosome 19p loci 5 genes)/(average CNVs of chromosome 19q loci 5 genes)  $\geq 2$ . To validate this definition of 1p/19q codeletion, we used 6 oligodendroglial tumor samples and 2 glioblastoma (GBM) samples that had previously been tested by array-CGH. Representative data of our 48-gene NGS panels for detection of the 1p/19q codeletion are shown in Figure 2. No 1p/19q codeletions were observed in the GBM samples (100% specificity) and concordant positive results were obtained for all oligodendroglial samples (100% sensitivity) (Figures 2, S1 and S2). Thus, agreement was observed between both tests.

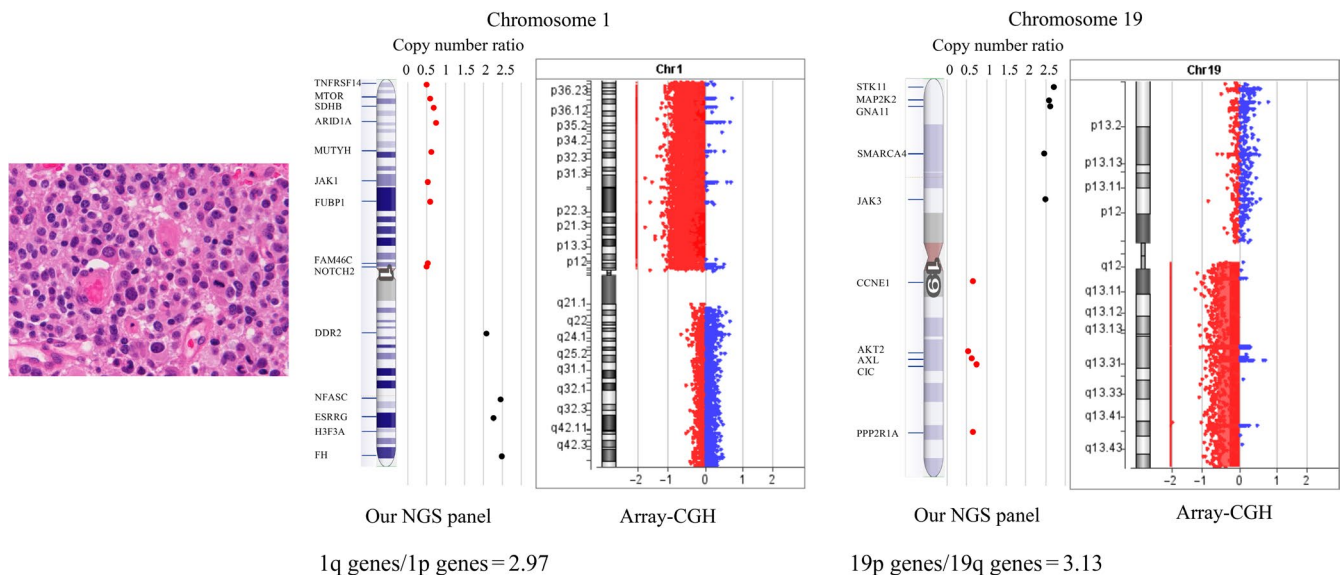


**FIGURE 2** Detection of 1p/19q codeletion. A patient with anaplastic oligodendrogloma with *IDH*-mutation and 1p/19q codeletion. For detection of 1p/19q codeletion, we analyzed copy number variations (CNVs) of chromosome 1p loci (9 genes), chromosome 1q loci (5 genes), chromosome 19p loci (5 genes), and chromosome 19q loci (5 genes). To validate 1p/19q codeletion detection, oligodendroglial tumor samples were tested by array-comparative genomic hybridization (CGH)

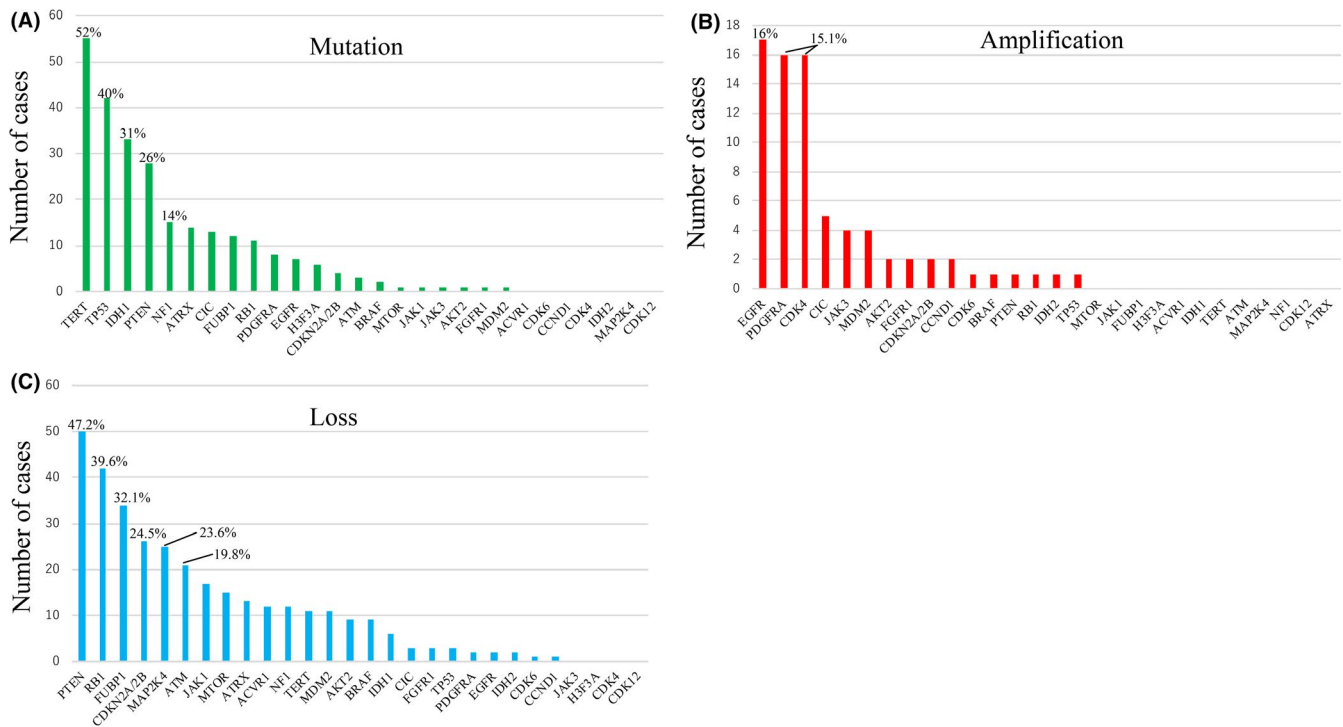


**FIGURE 3** Frequency of genetic alterations of all gliomas. Frequency of mutations (A), amplification (B), and loss (C) in each gene of glioma samples

### 3.2 | Mutation analysis in all gliomas

In total, we included 106 samples from 106 patients. The results of the NGS panel for the 106 samples were organized following the 2016 WHO classification system. The clinical data for each case are listed in Table S1. Table S2 summarizes the mutations and CNVs in all gliomas.

In 106 tumors, the most commonly mutated genes were *TERTp*, the tumor protein p53 gene (*TP53*), *IDH1*, *PTEN*, the neurofibromin 1 gene (*NF1*), and *ATRX* (Figure 3A). Interestingly, 6.6% (7/106) of cases showed no mutations in any of the regions examined by the NGS assay. No mutations were detected in 5.2% (3/58) of GBMs, 21.4% (3/14) of anaplastic astrocytomas, and 11.1% (1/9) of diffuse astrocytomas. *IDH1* mutations were identified in 33 of the 44 (75%) diffuse and anaplastic gliomas, including astrocytic and oligodendroglial tumors, as well as secondary GBMs. These mutations corresponded to *IDH1*-R132H, and no *IDH2* mutations were detected. *TERTp* mutations were most commonly detected in oligodendroglial tumors (OD II: 90%; AO III: 100%), followed by *IDH*-wildtype GBMs (58.9%) (Table S2). Codeletion of 1p/19q was detected in all oligodendroglial tumors. Mutations of *CIC* and the far upstream element binding protein 1 gene (*FUBP1*) were detected in 68.4% and 57.9%, respectively, of the oligodendroglial tumors with 1p/19q codeletion. The most commonly mutated genes in GBMs with wildtype *IDH* were *TERTp*, *TP53*, *PTEN*, the retinoblastoma (RB) transcriptional corepressor 1 gene (*RB1*), *NF1*, and the platelet derived growth factor receptor alpha gene (*PDGFRA*) (Figure S3A). In astrocytomas (WHO grade II/III), the incidence of *IDH1*, *TP53*, and *ATRX* mutations was

significantly higher, at 52.2%, 56.5%, and 47.8%, respectively. The majority of astrocytomas (WHO grade II/III) with an *IDH1* mutation also showed a *TP53* mutation (100%) and frequent *ATRX* mutations (83.3%). The incidence of *TERTp* and *EGFR* mutations in grade III astrocytomas was higher than those in grade II *TERTp* and *PTEN* mutations were more common in GBMs, than in grade II/III astrocytomas. However, there were fewer *EGFR* and *ATRX* mutations in GBMs than in grade II/III astrocytomas (Table S2). We identified mutations in the extracellular domain of *EGFR* in 100% (2/2) of GBMs. We also identified mutations in the extracellular domain and kinase domain of *EGFR* in 80% (4/5) and 20% (1/5) of grade II/III astrocytomas, respectively. In DMG cases, the most commonly mutated genes were *TP53* and *NF1*, while *TERTp* mutations were not detected (Table S2).

### 3.3 | Copy number analysis in all gliomas

All of the 106 cases (100%) showed evidence of CNVs in one of the NGS panel genes. The most common genes showing evidence of amplification were *EGFR*, *PDGFRA*, and the cyclin dependent kinase 4 gene (*CDK4*) (Figure 3B). The most common genes showing evidence of loss were *PTEN*, *RB1*, *FUBP1*, the cyclin dependent kinase inhibitor 2A/B gene (*CDKN2A/B*), the mitogen-activated protein kinase 4 gene (*MAP2K4*), and the ataxia telangiectasia-mutated (ATM) serine/threonine kinase gene (*ATM*) (Figure 3C). In *IDH*-wildtype GBM cases, the most common genes showing evidence of amplification were *EGFR*, *CDK4*, and *PDGFRA* (Figure S3B), while the most common genes showing evidences of loss were *PTEN*, *RB1*, *CDKN2A/B*,

ATM, MAP2K4, NF1 (Figure S3C). The representative mutual exclusivity was observed in the pairs of PDGFRA amplification/mutation and EGFR amplification/mutation. In contrast, only 4.3% and 0% of astrocytomas (WHO grades II/III) showed evidence of PDGFRA amplification or NF1 loss, respectively. EGFR and CDK4 amplification, and CDKN2A/B homozygous deletion occurred in grade III astrocytomas, but was not detected in any of the grade II astrocytomas. In DMG cases, the most common genes showing evidence of amplification were PDGFRA and FGFR, while the most common genes showing evidences of loss were RB1, MAP2K4, PTEN, ATM, and NF1 (Table S2).

### 3.4 | Unsupervised hierarchical cluster analysis of all gliomas

To investigate the potential of the NGS panel data to molecularly classify tumors, we performed an unsupervised hierarchical cluster analysis taking into account sequence changes and CNVs detected in the 106 investigated gliomas. This analysis revealed 3 distinct groups of gliomas with mutations in IDH1, TERTp, CIC, FUBP1, PTEN, TP53, and ATRX, 1p/19q codeletion, PTEN and RB1 loss, CDKN2A/B homozygous deletion, and EGFR, CDK4, and PDGFRA amplification. One major cluster consisted of 61 primarily astrocytomas characterized predominantly by mutations of TERTp, PTEN, and ATRX, loss of PTEN and RB1, and amplification of EGFR. A second major cluster, including 26 primarily astrocytomas, was characterized by mutations in IDH1, ATRX, TP53, and PDGFRA, as well as amplification of CDK4 and PDGFRA. The third major cluster, including 19 primarily oligodendroglial tumors, was characterized by mutations in IDH1, TERTp, FUBP1, and CIC, as well as 1p/19q codeletion (Figure S4).

### 3.5 | Genetic and clinical features of wildtype IDH GBM

We identified 56 IDH-wildtype cases of GBM with available molecular data. Among this cohort, the average age of patients was 63.35 y old (range: 22-88). Genetic alterations in TERTp were detected in 33 tumors (58.9%) and the remaining 23 patients (41.1%) had TERTp-wildtype GBM. Importantly, the average age of patients with TERTp-wildtype and TERTp-mutant GBMs was not significantly different (62.87 vs 63.69 y,  $P = .426$ ). We examined the genetic correlation between TERTp-wildtype vs mutant tumors (Table 1). PDGFRA mutations and amplification were more common in TERTp-wildtype GBMs (10/23, 43%) than in TERTp-mutant GBMs (2/33, 6%). Conversely, EGFR mutations and amplification were more commonly seen in TERTp-mutant GBMs (11/33, 33%) than in TERTp-wildtype GBMs (3/23, 13%). We noted that 7/23 (30%) of the TERTp-wildtype GBMs harbored CDK4 amplification, compared with 5/33 (15%) of TERTp-mutant GBMs. Moreover, PTEN mutations and/or loss were detected in 29/33 (88%) of TERTp-mutant GBMs, while only 13/23 (57%) of TERTp-wildtype GBMs had PTEN mutation and/or loss (Table 1).

**TABLE 1** Comparison of IDH-wildtype glioblastomas according to TERT promoter mutation status

	TERTp-wild (n = 23)	TERTp-mutant (n = 33)	P-value
MTOR	1 (4%)	0 (0%)	.179
JAK1	1 (4%)	0 (0%)	.179
FUBP1	1 (4%)	0 (0%)	.179
PDGFRA mutation and/or amplification	10 (43%)	2 (6%)	.001*
EGFR mutation and/or amplification	3 (13%)	11 (33%)	.076
BRAF	1 (4%)	0 (0%)	.179
CDKN2A + CDKN2B mutation and/or homozygous deletion	9 (39%)	14 (42%)	.805
PTEN mutation and/ or loss	13 (57%)	29 (88%)	.008*
ATM	1 (4%)	0 (0%)	.179
CDK4 amplification	7 (30%)	5 (15%)	.173
MDM2 amplification	1 (4%)	2 (6%)	.777
RB1 mutation and/ or loss	12 (52%)	19 (58%)	.689
TP53 mutation and/ or loss	13 (57%)	14 (42%)	.298
NF1 mutation and/ or loss	5 (22%)	10 (30%)	.473
ATRX loss	2 (9%)	6 (18%)	.306

Note: Groups were compared by chi-square ( $\chi^2$ ) tests.

\* $P < .05$  was considered statistically significant.

Next, we performed an unsupervised hierarchical cluster analysis on the 56 IDH-wildtype GBMs. This analysis revealed 3 distinct groups of IDH-wildtype GBMs, with mutations in TERTp, PTEN, RB1, NF1, TP53, and PDGFRA, loss of PTEN, RB1, and NF1, homozygous deletion of CDKN2A/B, as well as EGFR, CDK4, and PDGFRA amplification. One major cluster (Group A) was characterized by mutations of TERTp and NF1, loss of PTEN and NF1, amplification of EGFR, and a lack of TP53 mutations. A second major cluster (Group B) was characterized by mutations in TERTp, PTEN, TP53, and RB1 as well as a lack of CDKN2A/B homozygous deletion. The third major cluster (Group C) was characterized by mutations in TP53 and PDGFRA, amplification of CDK4 and PDGFRA, homozygous deletion of CDKN2A/B, and a lack of TERTp and PTEN mutations (Figure 4).

In addition, we compared clinical features among Groups A, B, and C (Table 2). The average Ki-67 score of Group C was 45.17%, which was significantly higher than that of Group A ( $P = .007$ ) but similar to that of Group B (Table 2). Although there was a trend for patients in Group C toward a periventricular tumor location, there was no statistical significance ( $P = .073$ ). We did not detect any differences in gender and Karnofsky performance status. The average age of Group C was 71.4, meaning these patients were significantly

older than that of Groups A and B ( $P = .021$ ). Interestingly, when we excluded Group C, the average age of patients with *TERT*<sub>p</sub>-wildtype GBMs was 48.56 y, which was significantly younger than that of patients with *TERT*<sub>p</sub>-mutant GBMs (63.75 y,  $P = .009$ ). The median time of overall survival was 65 mo for Group A, 13 mo for Group B, and 19 mo for Group C. The overall survival was significantly shorter in Groups B and C compared with that in Group A ( $P = .012$ ) (Figure S5A). Moreover, the overall survival was not significantly different when we compared *TERT*<sub>p</sub>-wildtype and *TERT*<sub>p</sub>-mutant statuses ( $P = .298$ ) (Figure S5B). However, when we excluded Group C from this analysis, the survival was significantly shorter for patients with *TERT*<sub>p</sub>-mutant GBM, compared with that for patients with *TERT*<sub>p</sub>-wildtype GBM ( $P = .042$ ) (Figure S5C).

### 3.6 | Validation of *PDGFRA* gene amplification by FISH

To validate *PDGFRA* gene amplifications performed by our NGS panel, we conducted FISH on 10 selective GBM cases, comprising 5 defined by NGS as showing *PDGFRA* amplification, and 5 defined as lacking *PDGFRA* amplification. FISH analysis showed that there was no *PDGFRA* amplification in the GBM samples defined by NGS as lacking *PDGFRA* amplification, and concordant positive results in

GBM samples defined by NGS as showing *PDGFRA* amplification (Figure S6).

### 3.7 | *EGFR* and *PDGFRA* alterations in large validation cohort

We retrieved molecular characteristics of the GBM cohort from a previous publication,<sup>29</sup> and having excluded *H3F3A*, *IDH1/2* and *BRAF* V600E-mutant cases, we analyzed 468 cases conclusively diagnosed as *IDH*-wildtype GBM using cBioPortal for Cancer Genomics (<https://cbioportal.org>). Genetic alterations in *TERT*<sub>p</sub> were detected in 89% of *IDH*-wildtype GBM. Mutual exclusivity was observed in the pairs of *PDGFRA* alterations and *EGFR* alterations (Figure S7).

## 4 | DISCUSSION

In this study, we constructed a glioma-tailored 48-gene NGS panel for detecting 1p/19q codeletion and driver gene mutations as a routine molecular diagnostic tool for gliomas in a single platform. Zacher et al and Na et al reported that 1p/19q codeletion could be detected by their NGS panels.<sup>20,22</sup> However, their panels did not include whole chromosome arms (1p and 19q) and did not allow for

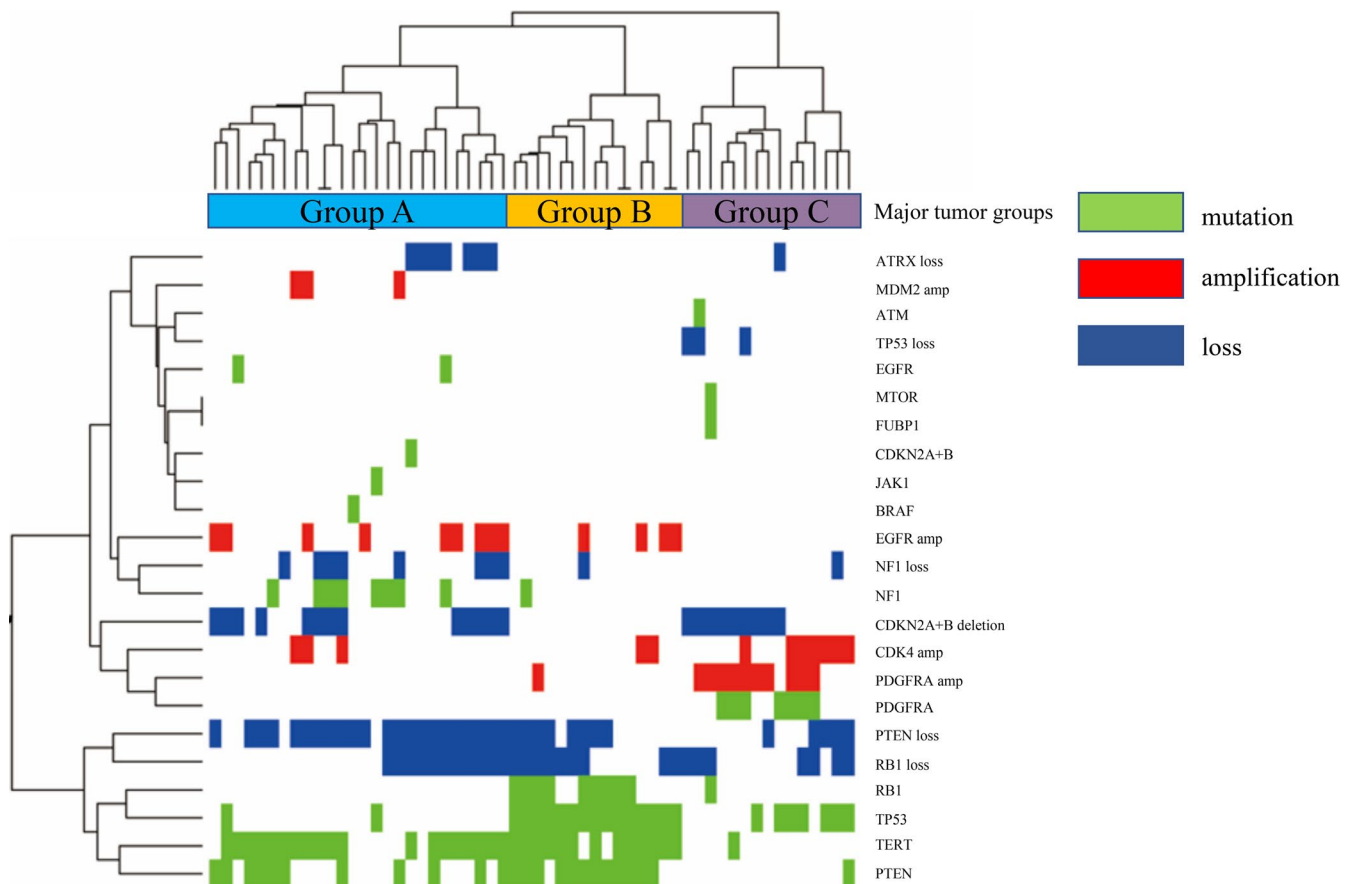


**FIGURE 4** Results of unsupervised hierarchical clustering analysis of the glioma-tailored 48-gene next-generation sequencing (NGS) panel data obtained in 56 *IDH*-wildtype glioblastomas

**TABLE 2** Clinical features of *IDH*-wildtype glioblastomas according to subtypes by unsupervised hierarchical cluster analysis

	Group A (n = 26)		Group B (n = 15)		Group C (n = 15)		P-value
	Cases	Ratio (%)	Cases	Ratio (%)	Cases	Ratio (%)	
Age	58.04 ± 15.81		64.53 ± 15.34		71.4 ± 10.26		.021*
Gender							
Male	15	57.69	8	53.33	8	53.33	.948
Female	11	42.31	7	46.67	7	46.67	
Location							
Periventricular	8	30.77	4	26.67	10	66.67	.073
Subcortical	17	65.38	11	73.33	5	33.33	
Infratentorial	1	3.85	0	0	0	0	
Karnofsky performance status							
0-70	7	26.79	7	46.67	7	46.67	.309
80-100	19	73.08	8	53.33	8	53.33	
Ki-67 (%)	30.08 ± 11.33		45.4 ± 19.69		45.17 ± 22.50		.007*
Representative genetic features							
<i>TERTp</i>	Mutant		Mutant		Wild		
<i>PDGFRA</i>	Intact		Intact		amp/mut		
<i>PTEN</i>	Mutant		Mutant		Wild		
<i>TP53</i>	Wild		Mutant		Mutant		
<i>CDKN2A/B</i>	Homozygous deletion		Intact		Homozygous deletion		

Note: Groups were compared by chi-square ( $\chi^2$ ) tests.

\* $P < .05$  was considered statistically significant.

the distinction between whole and partial chromosomal loss. In this study, we integrated the loss of heterozygosity from the CNV analysis of genes on chromosome 1p (9 genes), 1q (5 genes), 19p (5 genes), and 19q (5 genes) to identify the complete codeletion of 1p/19q. The copy number loss of 1p/19q genes detected in NGS was compared with CGH and the results were concordant in cases of oligodendroglial tumors. We believe that our method accurately detects 1p and 19q whole chromosome arm deletion. For the detection of diagnostic DNA copy number changes, our glioma-tailored 48-gene NGS panel reliably revealed complete 1p/19q codeletion.

Half of the *IDH*-wildtype grade II/III astrocytomas exhibited unfavorable genetic features such as alterations of *EGFR*, *PTEN*, *RB1*, and *TERTp* in our cohort study. Some of *IDH*-mutant grade II/III astrocytomas exhibited homozygous deletion of *CDKN2A/B* or amplification of *CDK4*. Moreover, a recent report suggested that homozygous deletion of *CDKN2A/B* and amplification of *PDGFRA* and *CDK4* are related to poor prognoses in *IDH*-mutant astrocytic gliomas.<sup>7,30,31</sup> Thus, our NGS panel offers feasible molecular stratifications for risk.

Recent reports have indicated that 70%-80% of GBM genomes harbor either C228T or C250T mutations in the promoter region of *TERT*.<sup>32-36</sup> The *IDH*-wildtype GBM bearing wildtype *TERTp* is associated with prolonged overall survival compared with those carrying mutations in *TERTp*.<sup>35-37</sup> In our cohort, 58.9% of *IDH*-wildtype GBM showed mutations in *TERTp*, which is substantially less frequent than in previous reports. However, another report from Japan indicated that 58%-59% of

GBM had mutations in *TERTp*,<sup>38,39</sup> suggesting that *TERTp* mutations may be less frequent in Japan than in other countries. Previous reports have shown that patients with the *TERTp*-wildtype GBM were significantly younger, on average, than those with *TERTp*-mutant GBM,<sup>34,36,40,41</sup> contrasting with our results. However, when we analyzed 301 cases conclusively diagnosed with *IDH*-wildtype GBM, part of a previously published Japanese large cohort,<sup>39</sup> the average age of patients with *TERTp*-wildtype and *TERTp*-mutant GBMs was statistically comparable (61.02 vs 63.36 y,  $P = .065$ ), in line with our findings.

Another study has shown that a portion of *IDH*- and *TERTp*-wildtype GBM utilizes distinct genetic mechanisms of telomere maintenance driven by an alternative lengthening of telomerase positive subgroup displaying alterations in *ATRX* or *SMARCAL1*, and *TERT* structural rearrangements.<sup>42</sup> However, our NGS panel could not detect *SMARCAL1* alteration and *TERT* structural variants, which constitutes a limitation of our NGS panel.

In this study, our analyses showed that the *TERTp*-wildtype subgroup of *IDH*-wildtype GBM had a distinct genomic profile, being significantly enriched for *PDGFRA* mutations and/or amplification compared with *TERTp*-mutant GBM. Moreover, *TERTp*-mutant GBMs are enriched for *PTEN* mutations and/or loss compared with *TERTp*-wildtype GBM. Approximately 15% of *IDH*-wildtype GBM had amplification of *PDGFRA*, which is compatible with our findings.<sup>38</sup> Recent reports have indicated that 14.4%-26% of GBM genomes harbor mutations in *EGFR*.<sup>8,43</sup> However, the frequency of *EGFR* mutations

in GBMs from our cohorts (3.4%) was much lower. This discrepancy may be due to the inclusion of a Japanese cohort.

Using hierarchical molecular classification of *IDH*-wildtype GBM, we revealed 3 distinct groups. One major cluster (Group C) was characterized by mutations in *TP53* and *PDGFRA*, amplification of *CDK4* and *PDGFRA*, homozygous deletion of *CDKN2A/B*, and a lack of *TERTp* and *PTEN* mutations. Interestingly, Group C was significantly associated with older age, despite the absence of *TERTp* mutations. No previous studies have reported the correlations between *TERTp*-wildtype status and *PDGFRA* alteration, thus we hypothesized that Group C in our cohort is a distinct subgroup of *IDH*-wildtype GBM. Interestingly, in our cohorts, there was no difference in the average age of patients with *TERTp*-wildtype GBM or *TERTp*-mutant GBM. However, when we excluded Group C, patients with *TERTp*-wildtype GBM were significantly younger than those with *TERTp*-mutant GBM, in accordance with previous studies.<sup>34,36,40,41</sup> No distinct difference in survival was observed for patients with *TERTp*-wildtype GBM or *TERTp*-mutant GBM in our cohorts. However, when we excluded Group C, survival was significantly shorter in patients with *TERTp*-mutant GBM than in patients with *TERTp*-wildtype GBM, in accordance with previous studies.<sup>35-37</sup> Therefore, the clinical characteristics of Group C might extend to a specific subgroup of Japanese cohorts. In addition, Group C was significantly associated with a higher Ki-67 score. In previous reports on GBMs, the Ki-67 score was significantly higher in tumors with *CDKN2A* homozygous deletions, which have a deleterious effect on cell cycle control.<sup>44</sup> We speculated that the high Ki-67 score of Group C might correlate with the dysregulation of cell cycles due to *CDKN2A/B* deletion and *CDK4* amplification. Moreover, Group C was significantly associated with poor prognosis. In previous reports, *PDGFRA* was defined as one of the molecular markers of GBM proneural subtypes. Curiously, *IDH*-wildtype proneural tumors had the worst prognosis among all GBM subtypes.<sup>8</sup> However, first-line bevacizumab plus standard-of-care therapy conferred a significant overall survival advantage for patients with proneural *IDH*-wildtype tumors.<sup>45</sup> Thus bevacizumab might be more effective in Group C than in other groups, which needs to be validated in a future study.

In summary, we report on the establishment of a glioma-tailored 48-gene NGS panel for detecting 1p/19q codeletion and driver mutations as a routine molecular diagnostic tool of gliomas. This study identified alterations of *PDGFRA* as co-occurring hallmarks of *TERTp*-wildtype GBM, potentially reflecting the unique molecular etiology and clinical features of these tumors. If further validated, our findings may have significant implications for the subclassification of *IDH*-wildtype GBM. Such subclassification are likely to provide more precise information to patients and may influence bedside decisions.

## DISCLOSURE

The authors declare no conflict of interest.

## ORCID

Akihide Tanimoto  <https://orcid.org/0000-0001-7508-1624>

Koji Yoshimoto  <https://orcid.org/0000-0001-7912-2024>

## REFERENCES

- Louis DN, Ohgaki H, Wiestler OD, Cavenee WK. *World Health Organization Histological Classification of Tumours of the Central Nervous System*. Lyon: International Agency for Research on Cancer; 2016.
- Louis DN, Ellison DW, Brat DJ, et al. cIMPACT-NOW: a practical summary of diagnostic points from Round 1 updates. *Brain Pathol*. 2019;29:469-472.
- Brat DJ, Aldape K, Colman H, et al. cIMPACT-NOW update 3: recommended diagnostic criteria for "Diffuse astrocytic glioma, *IDH*-wildtype, with molecular features of glioblastoma, WHO grade IV". *Acta Neuropathol*. 2018;136:805-810.
- Ellison DW, Hawkins C, Jones DTW, et al. cIMPACT-NOW update 4: diffuse gliomas characterized by MYB, MYBL1, or FGFR1 alterations or BRAFV600E mutation. *Acta Neuropathol*. 2019;137:683-687.
- Louis DN, Wesseling P, Paulus W, et al. cIMPACT-NOW update 1: Not Otherwise Specified (NOS) and Not Elsewhere Classified (NEC). *Acta Neuropathol*. 2018;135:481-484.
- Louis DN, Giannini C, Capper D, et al. cIMPACT-NOW update 2: diagnostic clarifications for diffuse midline glioma, H3 K27M-mutant and diffuse astrocytoma/anaplastic astrocytoma, *IDH*-mutant. *Acta Neuropathol*. 2018;135:639-642.
- Brat DJ, Aldape K, Colman H, et al. cIMPACT-NOW update 5: recommended grading criteria and terminologies for *IDH*-mutant astrocytomas. *Acta Neuropathol*. 2020;139:603-608.
- Brennan C, Verhaak R, McKenna A, et al. The somatic genomic landscape of glioblastoma. *Cell*. 2013;155:462-477.
- Cancer Genome Atlas Research Network. Comprehensive genomic characterization defines human glioblastoma genes and core pathways. *Nature*. 2008;455:1061-1068.
- Phillips HS, Kharbanda S, Chen R, et al. Molecular subclasses of high-grade glioma predict prognosis, delineate a pattern of disease progression, and resemble stages in neurogenesis. *Cancer Cell*. 2006;9:157-173.
- Capper D, Preusser M, Habel A, et al. Assessment of BRAF V600E mutation status by immunohistochemistry with a mutation-specific monoclonal antibody. *Acta Neuropathol*. 2011;122:11-19.
- Capper D, Zentgraf H, Balss J, Hartmann C, von Deimling A. Monoclonal antibody specific for *IDH1* R132H mutation. *Acta Neuropathol*. 2009;118:599-601.
- Rao S, Kanuri NN, Nimbalkar V, Arivazhagan A, Santosh V. High frequency of H3K27M immunopositivity in adult thalamic glioblastoma. *Neuropathology*. 2019;39:78-84.
- Cowell JK, Barnett GH, Nowak NJ. Characterization of the 1p/19q chromosomal loss in oligodendrogliomas using comparative genomic hybridization arrays (CGHa). *J Neuropathol Exp Neurol*. 2004;63:151-158.
- Buckley PG, Alcock L, Heffernan J, et al. Loss of chromosome 1p/19q in oligodendroglial tumors: refinement of chromosomal critical regions and evaluation of internexin immunostaining as a surrogate marker. *J Neuropathol Exp Neurol*. 2011;70:177-182.
- Nigro JM, Takahashi MA, Ginzinger DG, et al. Detection of 1p and 19q loss in oligodendrogloma by quantitative microsatellite analysis, a real-time quantitative polymerase chain reaction assay. *Am J Pathol*. 2001;158:1253-1262.
- Jeuken J, Cornelissen S, Boots-Sprenger S, et al. Multiplex ligation-dependent probe amplification: a diagnostic tool for simultaneous identification of different genetic markers in glial tumors. *J Mol Diagn*. 2006;8:433-443.
- Yoshimoto K, Iwaki T, Inamura T, et al. Multiplexed analysis of post-PCR fluorescence-labeled microsatellite alleles and statistical evaluation of their imbalance in brain tumors. *Jpn J Cancer Res*. 2002;93:284-290.
- Sim J, Nam D-H, Kim Y, et al. Comparison of 1p and 19q status of glioblastoma by whole exome sequencing, array-comparative

- genomic hybridization, and fluorescence in situ hybridization. *Med Oncol*. 2018;35:60.
20. Na K, Kim H-S, Shim HS, et al. Targeted next-generation sequencing panel (TruSight Tumor 170) in diffuse glioma: a single institutional experience of 135 cases. *J Neurooncol*. 2019;142:445-454.
  21. Tabone T, Abuhusain HJ, Nowak AK, Australian Genomics and Clinical Outcome of Glioma (AGOG) Network, Erber WN, McDonald KL. Multigene profiling to identify alternative treatment options for glioblastoma: a pilot study. *J Clin Pathol*. 2014;67:550-555.
  22. Zacher A, Kaulich K, Stepanow S, et al. Molecular diagnostics of gliomas using next generation sequencing of a glioma-tailored gene panel. *Brain Pathol*. 2017;27:146-159.
  23. Ballester LY, Fuller GN, Powell SZ, et al. Retrospective analysis of molecular and immunohistochemical characterization of 381 primary brain tumors. *J Neuropathol Exp Neurol*. 2017;76:179-188.
  24. D'Haene N, Meléndez B, Blanchard O, et al. Design and validation of a gene-targeted, next-generation sequencing panel for routine diagnosis in gliomas. *Cancers (Basel)*. 2019;11(6):773.
  25. Synhaeve NE, van den Bent MJ, French PJ, et al. Clinical evaluation of a dedicated next generation sequencing panel for routine glioma diagnostics. *Acta Neuropathol Commun*. 2018;6:126.
  26. Nikiforova MN, Wald AI, Melan MA, et al. Targeted next-generation sequencing panel (GlioSeq) provides comprehensive genetic profiling of central nervous system tumors. *Neuro-oncology*. 2016;18:379-387.
  27. Xu C, Nezami Ranjbar MR, Wu Z, et al. Detecting very low allele fraction variants using targeted DNA sequencing and a novel molecular barcode-aware variant caller. *BMC Genom*. 2017;18:5.
  28. Peng Q, Vijaya Satya R, Lewis M, et al. Reducing amplification artifacts in high multiplex amplicon sequencing by using molecular barcodes. *BMC Genom*. 2015;16:589.
  29. Jonsson P, Lin AL, Young RJ, et al. Genomic correlates of disease progression and treatment response in prospectively characterized gliomas. *Clin Cancer Res*. 2019;25:5537-5547.
  30. Shirahata M, Ono T, Stichel D, et al. Novel, improved grading system(s) for IDH-mutant astrocytic gliomas. *Acta Neuropathol*. 2018;136:153-166.
  31. Yang RR, Shi ZF, Zhang ZY, et al. IDH mutant lower grade (WHO Grade II/III) astrocytomas can be stratified for risk by CDKN2A, CDK4 and PDGFRA copy number alterations. *Brain Pathol*. 2020;30:541-553. <https://doi.org/10.1111/bpa.12801>
  32. Nguyen HN, Lie A, Li T, et al. Human TERT promoter mutation enables survival advantage from MGMT promoter methylation in IDH1 wild-type primary glioblastoma treated by standard chemoradiotherapy. *Neuro-oncology*. 2017;19:394-404.
  33. Spiegl-Kreinecker S, Lötsch D, Ghanim B, et al. Prognostic quality of activating TERT promoter mutations in glioblastoma: interaction with the rs2853669 polymorphism and patient age at diagnosis. *Neuro-oncology*. 2015;17:1231-1240.
  34. Eckel-Passow JE, Lachance DH, Molinaro AM, et al. Glioma groups based on 1p/19q, IDH, and TERT promoter mutations in tumors. *N Engl J Med*. 2015;372:2499-2508.
  35. Killela PJ, Reitman ZJ, Jiao Y, et al. TERT promoter mutations occur frequently in gliomas and a subset of tumors derived from cells with low rates of self-renewal. *Proc Natl Acad Sci USA*. 2013;110:6021-6606.
  36. Labussière M, Boisselier B, Mokhtari K, et al. Combined analysis of TERT, EGFR, and IDH status defines distinct prognostic glioblastoma classes. *Neurology*. 2014;83:1200-1206.
  37. Labussière M, Di Stefano AL, Gleize V, et al. TERT promoter mutations in gliomas, genetic associations and clinico-pathological correlations. *Br J Cancer*. 2014;111:2024-2032.
  38. Umehara T, Arita H, Yoshioka E, et al. Distribution differences in prognostic copy number alteration profiles in IDH-wild-type glioblastoma cause survival discrepancies across cohorts. *Acta Neuropathol Commun*. 2019;7:99.
  39. Arita H, Yamasaki K, Matsushita Y, et al. A combination of TERT promoter mutation and MGMT methylation status predicts clinically relevant subgroups of newly diagnosed glioblastomas. *Acta Neuropathol Commun*. 2016;4:79.
  40. Williams EA, Miller JJ, Tummala SS, et al. TERT promoter wild-type glioblastomas show distinct clinical features and frequent PI3K pathway mutations. *Acta Neuropathol Commun*. 2018;6:106.
  41. Yamashita K, Hatae R, Hiwatashi A, et al. Predicting TERT promoter mutation using MR images in patients with wild-type IDH1 glioblastoma. *Diagn Interv Imaging*. 2019;100:411-419.
  42. Diplas BH, He X, Brosnan-Cashman JA, et al. The genomic landscape of TERT promoter wildtype-IDH wildtype glioblastoma. *Nat Commun*. 2018;9:2087.
  43. Lee JC, Vivanco I, Beroukhi R, et al. Epidermal growth factor receptor activation in glioblastoma through novel missense mutations in the extracellular domain. *PLoS Med*. 2006;3:e485.
  44. Ono Y, Tamiya T, Ichikawa T, et al. Malignant astrocytomas with homozygous CDKN2/p16 gene deletions have higher Ki-67 proliferation indices. *J Neuropathol Exp Neurol*. 1996;55:1026-1031.
  45. Sandmann T, Bourgon R, Garcia J, et al. Patients with proneural glioblastoma may derive overall survival benefit from the addition of bevacizumab to first-line radiotherapy and temozolomide: retrospective analysis of the AVAglio trial. *J Clin Oncol*. 2015;33(25):2735-2744.

## SUPPORTING INFORMATION

Additional supporting information may be found online in the Supporting Information section.

**How to cite this article:** Higa N, Akahane T, Yokoyama S, et al. A tailored next-generation sequencing panel identified distinct subtypes of wildtype IDH and TERT promoter glioblastomas. *Cancer Sci*. 2020;111:3902-3911. <https://doi.org/10.1111/cas.14597>